Available online at www.sciencedirect.com
ScienceDirect
Bioorganic Chemistry 36 (2008) 113–120
BIOORGANIC CHEMISTRY
www.elsevier.com/locate/bioorg

# 5-Enolpyruvylshikimate-3-phosphate synthase: Determination of the protonation state of active site residues by the semiempirical method

Anivaldo Xavier de Souza [a], Carlos Mauricio R. Sant'Anna [b,*]

[a] *Colégio Técnico da Universidade Rural, Universidade Federal Rural do Rio de Janeiro (UFRRJ), BR 465 – km 7 (Antiga Rio-São Paulo, km 47), Seropédica, RJ 23890-000, Brazil*

[b] *Departamento de Química, ICE, Universidade Federal Rural do Rio de Janeiro (UFRRJ), BR 465 – km 7 (Antiga Rio-São Paulo, km 47), Seropédica, RJ 23890-000, Brazil*

Received 6 September 2007
Available online 5 March 2008

**Abstract**

EPSP synthase (EPSPS) catalyzes the addition of shikimate-3-phosphate (S3P) and phosphoenolpyruvate (PEP) to form a tetrahedral intermediate (TI) that is converted to 5-enolpyruvylshikimate-3-phosphate (EPSP) and inorganic phosphate. A semiempirical molecular modeling study of the EPSPS active site containing the TI was implemented for the assignment of the protonation states of four basic residues, Lys22, Lys340, His385, and Lys411, based on the evaluation of 16 different protonation states and comparison of the resulting energy minimized heavy atoms coordinates with available X-ray crystallographic data of the D313A mutant of EPSPS. The results, employing both gas phase and continuum solvent models, are indicative that after the TI formation the histidine residue is most probably in neutral form ($N^{\varepsilon}$-protonated) and the lysine residues are in protonated form, which suggests that none of the presently proposed assignments of aminoacid residues involved in the reaction mechanism could be completely correct. The protonated state of Lys22 in the presence of the TI supports the proposal that this residue is a general acid catalyst for TI breakdown. Modeling of the native enzyme active site suggests that Asp313 residue has only minor effects on the definition of the TI position inside the active site. Hydrogen-bonds distances suggest that, in order to act as a base, Asp313 needs the intermediacy of a hydroxyl group of the TI for effecting the attack on the TI methyl group in the elimination step leading to EPSP, as suggested previously in the literature.


*Keywords:* EPSP synthase; Active site residues; Protonation state; Semiempirical method

## 1. Introduction

The biosynthesis of 5-enolpyruvylshikimate-3-phosphate (EPSP) from the substrates shikimate-3-phosphate (S3P) and phosphoenolpyruvate (PEP), an essential reaction toward the biosynthesis of aromatic compounds in bacteria, fungi, algae, higher plants, and apicomplexan parasites, is catalyzed by the enzyme EPSP synthase (EPSPS), also called AroA [1]. Because this biosynthetic route is absent from mammals, this reaction is an attractive target for the development of antimicrobial and herbicide compounds. The widely used weed control agent glyphosate (*N*-(phosphonomethyl)glycine)) is a competitive inhibitor of EPSPS [2], which acts by forming a non-covalent but stable ternary complex with the enzyme and S3P [3].

Rational inhibitor design could benefit from a detailed understanding of the EPSPS catalyzed reaction mechanism, which have implications in crop production and human health. Although a reaction mechanism involving an intermediate species covalently bound to the enzyme has been proposed [4,5], several experimental results support the presently accepted addition–elimination mechanism with a tetrahedral intermediate (TI) composed by

* Corresponding author. Fax: +55 21 2682 1872.
*E-mail address:* santanna@ufrrj.br (C.M.R. Sant'Anna).

0045-2068/$ - see front matter © 2008 Elsevier Inc. All rights reserved.
doi:10.1016/j.bioorg.2007.12.007

the two substrates covalently linked to each other [6–8] (Fig. 1), especially the TI trapping in the D313A mutant of *Escherichia coli* EPSPS followed by a detailed depiction of the co-crystallized structure [9].

Many efforts have been implemented for the assignment of the aminoacid residues involved in the proton transfers in the reaction mechanism. Kinetic studies on site-directed mutants [10], partitioning analysis [11], solid state NMR [12], and X-ray crystallography studies of the complex of EPSPS with S3P and glyphosate [3] and of the mutant EPSPS containing the TI [9] are examples of experimental techniques employed to identify the catalytically most important residues, but some conclusions from these studies remain controversial. For example, Berti and co-workers concluded that there are no aminoacid residues that catalyze solely addition or elimination and that Glu341 (in neutral form) was the proton donor in the intermediate formation and the proton acceptor in the elimination of the intermediate, while Lys22 was the proton acceptor from S3P in the first step and a general acid catalyst for phosphate elimination in the second step [11]. The location of Lys22 is suitable for protonating the bridging phosphate oxygen in the THI PEP moiety, which was demonstrated to be an effective catalytic strategy to promote THI breakdown in non-enzymatic model reactions [13]. On the other hand, Schönbrunn and co-workers suggested that Lys22 was able to accomplish the two proton transfers required for the addition, first as a base abstracting the H atom of S3P, later as an acid protonating the C3 atom of PEP; Asp313 was proposed as the base for proton abstraction from the reaction intermediate because the overall addition–elimination reaction is halted after the addition step as a consequence of its mutation to an alanine residue [9].

This controversy may be clarified by the definition of the protonation state of the enzymatic active site residues. The crystallographic structure of the TI-containing EPSPS is known from the work of Eschenburg et al., but hydrogen atoms positions cannot be usually determined by an X-ray diffraction technique. The p$K_a$ of basic residues, such as lysine and histidine, could be influenced by the adjacent microenvironment, including the presence of neighboring acidic and/or charged residues, and residues containing polarizable electron-rich groups, such as the rings of aromatic residues. In the absence of experimental information, computational methods can be explored for estimation of protonation states as it was shown, for example, by the use of a molecular mechanics method by Signorini et al. for the prediction of the protonation state of histidine residues buried in the protein core [14], and by González-Nilo et al., who have determined by means of DFT and FEP calculations the protonation state of lysine residues of the phosphoenolpyruvate carboxykinase active site [15].

The use of EPSPS-catalyzed reaction mechanisms as a tool for the rational design of new herbicide leads is clearly dependent on the correct definition of the protonation state of active site basic residues. In the present work, we describe a semiempirical molecular modeling study for the assignment of the protonation states of all basic residues in the EPSPS active site containing the reaction intermediate, based on the evaluation of the different protonation possibilities and comparison of the resulting energy minimized heavy atom positions with those

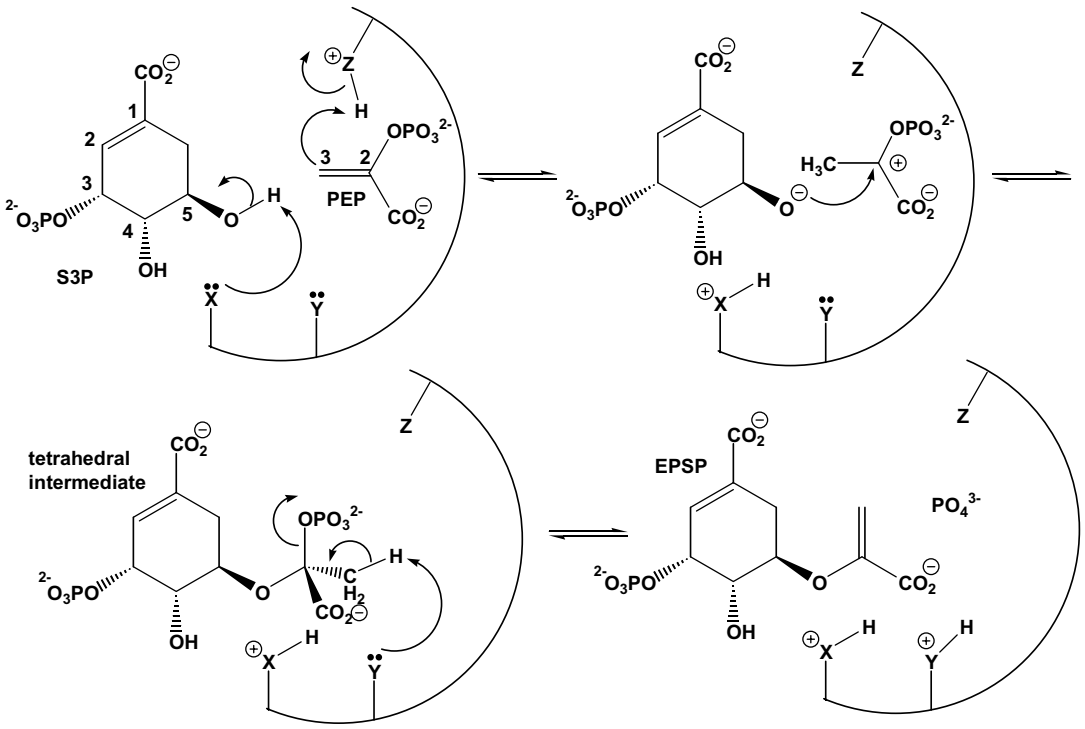


Fig. 1. Possible mechanism of EPSP synthase catalyzed reaction.

observed in the X-ray crystallographic structure of *E. coli* D313A mutant of EPSPS [9]. These results are complemented by a study of the influence of protonation state on the TI-containing native EPSPS active site.

## 2. Methodology

In order to choose the best semiempirical method for the calculations, we carried out a preliminary study on a hydrogen-bonded complex between methylamine and methylphosphate, as a simple model of the interaction between the lysine side chain and the TI phosphate groups. The geometries were optimized with AM1 [16] and PM3 [17,18] Hamiltonians and also at the *ab initio* HF/6-311+G** level with Spartan'02 for Linux (Wavefunction, Inc.). In the AM1 minimum energy structure, a bifurcated conformation with each of the hydrogen atoms of the methylamine amino group making hydrogen-bonds with an oxygen atom of the methylphosphate molecule was obtained, a result that does not correspond to the *ab initio* minimum, which contains only one, shorter, hydrogen-bond between the amino and the phosphate groups. On the other hand, the optimized PM3 geometry was very similar to the *ab initio* minimum, in accordance with literature results, which showed that PM3 correctly predicts the structure of many types of intermolecular hydrogen-bonds [19–22].

As a simple test of the PM3 method reliability for evaluation of the protonation states of histidine and lysine residues in a protein environment, modeling results were compared with available neutron diffraction results of two selected proteins: D-xylose isomerase at 2.2 Å resolution (entry 2GVE of the Protein Data Bank, PDB) [23] and β-trypsin at 1.8 Å resolution (entry 1NTP of the PDB) [24]. The neutron scattering properties provide a method for locating hydrogen atoms by introducing deuterium into the protein and for identifying which hydrogen atoms are readily replaced by deuterium and the extent of this replacement. Neutron diffraction data at ~2 Å resolution can unambiguously define hydrogen atom positions. Input files for the semiempirical calculations were prepared from the PDB files by selection of aminoacid residues and water molecules in close contact with three reference aminoacid residues: the D-xylose isomerase Lys149 residue, and β-trypsin His40 and His57 residues. Atomic coordinates were selected with the Rasmol 2.6 program [25]; conversion of the selected PDB files to the internal coordinates Mopac input files and addition of hydrogen atoms were implemented by means of the Babel 1.6 program [26]. Calculations were done with the Mopac 6.0 [27] program and the results obtained with the PM3 method, discussed in the next section, compared well with the experimental data.

The EPSPS protonation state study was based on entry 1Q36 (PDB), which describes the X-ray structure of the tetrahedral reaction intermediate state of D313A mutant of *E. coli* EPSPS [9]. According to the partitioning analysis implemented by Myzied et al., at least eight mutations of EPSPS residues caused a >1000-fold decrease in specific activity, demonstrating that a large number of residues are important for transition state stabilization, characterizing an "ensemble catalysis", in contrast to some enzymes where a single amino acid can be responsible for the catalytic enhancement [11]. The selected working models were composed by the residues and water molecules with at least one atom located inside a 6 Å radius sphere around the co-crystallized TI, which encompass all residues and water molecules making direct contacts with it: Lys22, Ser23, Val24, Arg27, Asp49, Asn94, Ala95, Gly96, Thr97, Ala98, Arg100, Met121, Arg124, Val168, Ser169, Ser170, Gln171, Thr174, Val196, Ser197, Tyr200, Ile203, Thr204, Pro312, Asp313, Met316, Asn336, Lys340, Glu341, Arg344, Asp384, His385, Arg386, Lys411, Thr412, and eight water molecules. We think that a quantum-mechanical model is the most adequate one to describe the complex interactions in the EPSPS selected active site, since it contains a number of potentially charged and polarizable species in close contact. Because there is a great number of atoms in the structure and various structures to evaluate, we chose for the calculations the semiempirical molecular orbital method with the linear scaling approach [28], which enables fast quantum calculations on systems composed of many hundreds of atoms. We have recently used the same procedure for the investigation of enzymatic mechanisms associated to a pesticide mechanism of action [29] and pesticide lead development [30].

All EPSPS model optimizations were carried out in the "gas phase" with PM3, as implemented in the Mopac2002 program [Fujitsu, Inc.] for Linux. After coordinates selection and conversion to Mopac input files, the resulting files were edited for addition of hydrogen atoms to the water oxygen atoms after a careful analysis in order to establish as many hydrogen-bonds as possible with the nearest hydrogen-bond acceptor atoms. All different combinations of protonation states of the four basic residues, His385, Lys22, Lys340, and Lys411, were finally prepared by suitable edition of the input files, resulting in 16 initial geometries, all containing more than 650 atoms. Arginine residues were considered in protonated form and aspartic acid and glutamic acid residues and the THI phosphate and carboxylate groups were considered in unprotonated form in all models. Solvent effects were accounted for implicitly by means of the conductor-like screening model (COSMO) [31] available in Mopac2002. Geometries were optimized with the Eigenvector Following routine to a gradient norm <1.0 kcal/(Å or rad).

## 3. Results and discussion

### 3.1. Comparison of neutron diffraction data and PM3 modeling results

Tables 1 and 2 present the comparison of the PM3 modeling results with the neutron diffraction data for lysine and

Table 1
Comparison of PM3 optimized structure and neutron diffraction data (PDB code 2GEV)

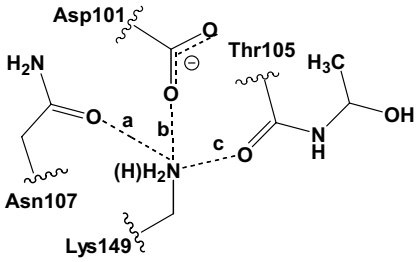


| Distance[a] | Experimental[b] | Protonated Lys149 | Neutral Lys149 | Neutral Lys149 | Neutral Lys149 |
|---|---|---|---|---|---|
| a | 2.58 | 2.77 | 5.85 | 3.58 | 3.94 |
| b | 2.98 | 2.74 | 3.69 | 4.65 | 2.82 |
| c | 2.99 | 2.79 | 2.85 | 3.83 | 3.42 |

[a] Distances are presented in Angstrom.
[b] Ref. [23].

Table 2
Comparison of PM3 optimized structure and neutron diffraction data (PDB code 1NTP)

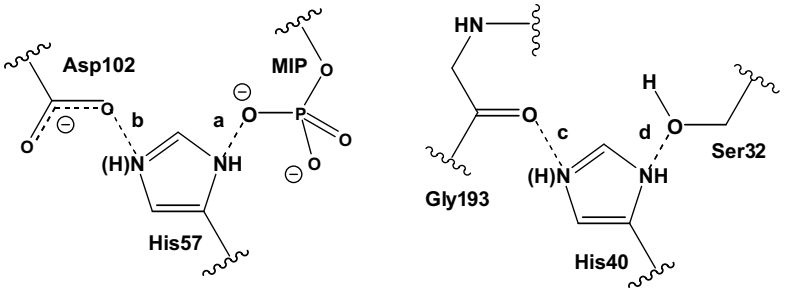


| Distance[a] | Experimental[b] | Protonated H57 | Neutral H57 ($N^{\varepsilon}$) | Neutral H57 ($N^{\delta}$) | Protonated H40 | Neutral H40 ($N^{\varepsilon}$) | Neutral H40 ($N^{\delta}$) |
|---|---|---|---|---|---|---|---|
| a | 2.63 | 2.72 | 3.35 | 4.37 | | | |
| b | 2.48 | 2.69 | 3.64 | 2.80 | | | |
| c | 2.67 | — | — | — | 2.84 | 2.89 | 3.89 |
| d | 2.59 | — | — | — | 2.76 | 2.74 | 3.31 |

[a] Distances are presented in Angstrom.
[b] Ref. [24].

histidine residues. In both experimental structures, we selected residues buried in the protein core because they are in a more similar environment to that of the EPSPS active site. The 2GEV Lys149 residue was chosen because it is near both neutral and charged residues. As can be observed in Table 1, the modeled distances between the side chain nitrogen atom and the hydrogen-bond acceptor atoms are much more closer to the experimental ones when the nitrogen atom is in the protonated form than when it is in the neutral form. The conclusion based on the modeling results is that the Lys149 residue should be in the protonated form, in accordance with the number of protons observed in the neutron diffraction structure.

Two histidine residues were selected from the 1NPT structure, His40, which is close to neutral residues, and His57, which is near anionic species, a carboxylate and a phosphate group. Three histidine possible states were considered: two neutral forms with either the $N^{\varepsilon}$ or $N^{\delta}$ nitrogen atom protonated, and one positively charged form with both $N^{\varepsilon}$ and $N^{\delta}$ atoms protonated. In the case of His57, there is a better resemblance between the modeled and the experimental distances when the residue is in cationic form. Once again, the PM3 modeling protonation state prevision agrees with the neutron diffraction data. However, for the His40 residue, both the cationic form (which is the correct state according to the neutron diffraction structure) and the neutral form with a hydrogen atom attached to the $N^{\varepsilon}$ atom lead to results similar to the experimental distances, so it was not possible to define unambiguously the protonation state of this residue by the modeling procedure.

### 3.2. EPSPS active site protonation state

The different protonation stares evaluated during the modeling procedure are summarized in Table 3.

Table 3
Protonation states of key structural features considered for comparison of EPSPS modeled and experimental structures

| Model | His385 | Lys22 | Lys340 | Lys411 |
|---|---|---|---|---|
| EPSPS1 | Protonated | Neutral | Neutral | Neutral |
| EPSPS2 | Neutral | Neutral | Neutral | Neutral |
| EPSPS3 | Neutral | Neutral | Neutral | Protonated |
| EPSPS4 | Protonated | Neutral | Neutral | Protonated |
| EPSPS5 | Protonated | Protonated | Neutral | Neutral |
| EPSPS6 | Neutral | Protonated | Neutral | Neutral |
| EPSPS7 | Neutral | Protonated | Neutral | Protonated |
| EPSPS8 | Protonated | Protonated | Neutral | Protonated |
| EPSPS9 | Protonated | Neutral | Protonated | Neutral |
| EPSPS10 | Neutral | Neutral | Protonated | Neutral |
| EPSPS11 | Neutral | Neutral | Protonated | Protonated |
| EPSPS12 | Protonated | Neutral | Protonated | Protonated |
| EPSPS13 | Protonated | Protonated | Protonated | Neutral |
| EPSPS14 | Neutral | Protonated | Protonated | Neutral |
| EPSPS15 | Neutral | Protonated | Protonated | Protonated |
| EPSPS16 | Protonated | Protonated | Protonated | Protonated |

As a criterion for identification of the most adequate description of the protonation states, some key structural features were chosen for comparison with the experimental values. The structural features explored for determination of the protonation state of His385 were the distance between its $N^{\delta}$ atom and the $O^{\gamma}$ atom of Thr412, and the distance between the His385 $N^{\varepsilon}$ atom and one of carboxylate oxygen atoms of Glu341 side chain. As can be observed in Table 4, this distance to the $O^{\gamma}$ atom of Thr412 is too short in the models where the $N^{\delta}$ atom was protonated; the models that better reproduce the experimental distance are those containing His385 in the neutral form. In fact, when unprotonated, the His385 $N^{\delta}$ atom is a hydrogen-bond acceptor from Thr412, but in the protonated form it is a hydrogen-bond donator to Thr412 $O^{\gamma}$ atom. As can be seen by the mean values presented on Table 4, of all analyzed structural features, this one has the least difference between the protonated and the unprotonated models.

Table 4
Key structural features considered for comparison of EPSPS modeled and experimental structures

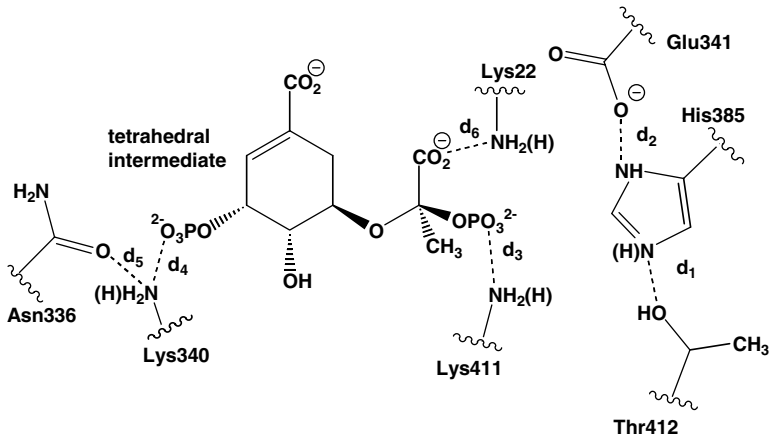


| Model[a] | $d_1$[b] | $d_2$ | $d_3$ | $d_4$ | $d_5$ | $d_6$ |
|---|---|---|---|---|---|---|
| 1 | ***2.72*** | ***2.45*** | 3.91 | 2.82 | 3.80 | 3.81 |
| 2 | 2.80 | 2.54 | 3.46 | 3.42 | 3.58 | 3.74 |
| 3 | 2.76 | 2.68 | ***2.72*** | 2.82 | 3.80 | 4.10 |
| 4 | *2.69* | ***2.61*** | ***2.70*** | 2.82 | 3.68 | 4.13 |
| 5 | ***2.71*** | ***2.45*** | 3.78 | 3.53 | 3.48 | ***2.81*** |
| 6 | 2.78 | 2.59 | 4.08 | 3.48 | 3.50 | ***2.79*** |
| 7 | 2.75 | 2.68 | ***2.71*** | 2.83 | 3.66 | ***2.81*** |
| 8 | ***2.70*** | ***2.61*** | ***2.69*** | 2.81 | 3.54 | ***2.81*** |
| 9 | ***2.70*** | ***2.47*** | 4.06 | ***2.66*** | ***2.76*** | 3.93 |
| 10 | 2.78 | 2.57 | 4.15 | ***2.66*** | ***2.77*** | 3.81 |
| 11 | 2.76 | 2.70 | ***2.72*** | ***2.65*** | ***2.76*** | 4.16 |
| 12 | ***2.67*** | ***2.62*** | ***2.71*** | ***2.64*** | ***2.75*** | 3.96 |
| 13 | ***2.71*** | ***2.48*** | 4.03 | ***2.66*** | ***2.75*** | ***2.80*** |
| 14 | 2.77 | 2.58 | 4.08 | ***2.66*** | ***2.76*** | ***2.80*** |
| 15 | 2.74 | 2.70 | ***2.72*** | ***2.65*** | ***2.74*** | ***2.82*** |
| 16 | ***2.69*** | ***2.63*** | ***2.70*** | ***2.66*** | ***2.73*** | ***2.82*** |
| Mean protonated | ***2.70*** | ***2.54*** | ***2.71*** | ***2.66*** | ***2.75*** | ***2.81*** |
| Mean unprotonated | 2.77 | 2.74 | 3.94 | 3.07 | 3.63 | 3.96 |
| 15w[c] | 2.78 | 2.68 | 2.64 | 2.72 | 2.71 | 2.76 |
| Experimental | 2.80 | 2.71 | 2.88 | 2.62 | 2.89 | 2.66 |

[a] Bold-italic entries correspond to protonated (cationic) residues.
[b] Distances are presented in Angstrom.
[c] Model 15 optimized with the COSMO water continuum model.

This result combined with the previous comparison with 1NPT His40 diffraction data makes doubtful the conclusion about the actual protonation state of this residue. The difference between the protonated and the unprotonated models is greater for the distance between His385 and Glu341 and is indicative of an unprotonated residue. It must also be remembered that one of the residues adjacent to His385 is an arginine residue (Arg386), which should be protonated due to its strongly basic guanidine side chain. This situation is expected to result in an unfavorable environment for a protonated histidine residue because of the electrostatic repulsion between the positive-charged side chains of both residues. In fact, it was observed that the conformation of the side chain of Arg386 is better represented in the models where His485 is in neutral form, as is exemplified in Fig. 2. Based on this analysis, we propose that the more probable protonation state of His385 is a neutral state with a protonated $N^{\varepsilon}$ atom.

In the EPSPS X-ray crystal structure, the side chain of Lys411 is close to the phosphate group of the TI PEP moiety, which is indicative of a hydrogen-bond between these groups. Although the hydrogen-bonding interaction between the $N^{\zeta}$ atom of the protonated lysine and the phosphate oxygen is somewhat overestimated by PM3 (Table 4), the calculated distance is much more closer to the experimental value than in the models where Lys411 is in neutral form, where the distances are too long in comparison to the experimental value, indicating that this residue should be in the protonated form when the enzyme contains the TI.

There are four potential hydrogen-bond acceptors in the surroundings of Lys340 $N^{\zeta}$ atom: the hydroxyl group connected to C4 ($N^{\zeta}$(Lys340)–O(hydroxyl) distance: 3.04 Å), the phosphate group attached to C3 ($N^{\zeta}$(Lys340)–O(phosphate) distance: 2.62 Å), a water molecule ($N^{\zeta}$(Lys340)–O($H_2O$104) distance: 3.06 Å), and, finally, the carbonyl group of the Asn336 side chain ($N^{\zeta}$(Lys340)–$O^{\delta}$(Asn336) distance: 2.90 Å). The two smaller distances were chosen as the structural features for comparison between calculated and theoretical data. The analysis of both distances lead to consistent results (Table 4), which are indicative that the models unprotonated at Lys340 are not able to adequately represent the experimental structure at this point, leading to longer $N^{\zeta}$(Lys340)–O(phosphate) and $N^{\zeta}$(Lys340)–$O^{\delta}$(Asn336) distances than the experimental ones.

From the analysis of the crystallographic data, hydrogen-bonding interactions are expected between the Lys22 $N^{\zeta}$ atom and a carboxylate oxygen atom of the TI PEP moiety. Based on the analysis of this structural feature, it can be observed that in all models where the Lys22 residue is unprotonated, the distance is too long in comparison to the experimental data (Table 4). The overall analysis indicates that model 15 is the model that most adequately fits to all evaluated structural features, which corresponds to an active site holding a neutral histidine residue and three protonated lysine residues (Fig. 3). In order to eliminate the possibility of this result as an artifact of the "gas phase" modeling, this same model was energy minimized with the COSMO water continuum model. As can be seen in Table 4 (model 15w), the results are in qualitative accordance with the "gas phase" results, leading to the same conclusion about the protonation state of the basic aminoacid residues.

### 3.3. Evaluating the effect of the protonation state in the native EPSPS active site

How the predicted protonation state would influence the native active site? To answer this question we substituted

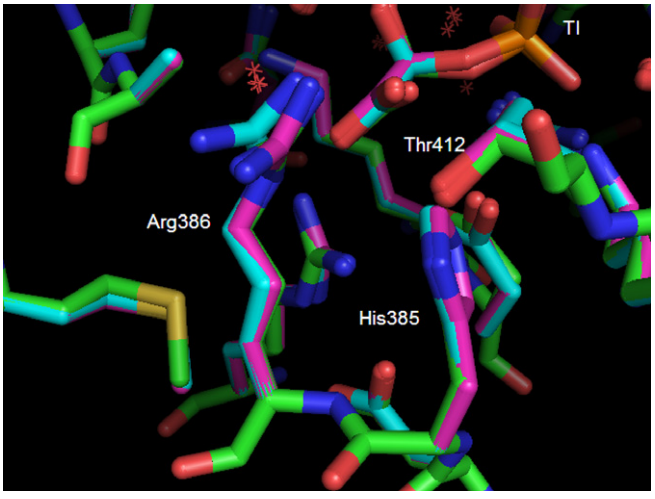


Fig. 2. Superposition of 1Q36 X-ray structure [9], and optimized models 15 (unprotonated His385 residue) and 16 (protonated His385 residue). Hydrogen atoms were omitted to improve clarity. Color code: green, C (1Q36); magenta, C (model 15); cyan, C (model 16); red, O; blue, N; orange, P; yellow, S.

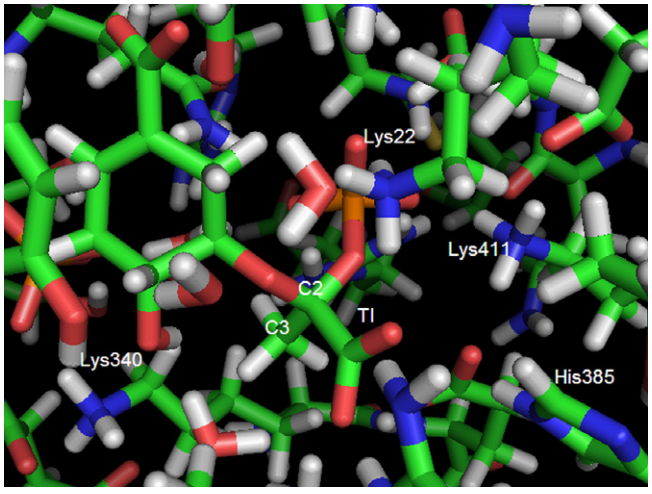


Fig. 3. 3D representation of optimized model 15, showing the protonation state of the basic residues evaluated in this work. The labeled carbon atoms refer to C2 and C3 atoms of the PEP moiety. Color code: green, C; white, H; red, O; blue, N; orange, P.

aspartate for the mutant Ala313 residue in model 15 and also in model 16, because of the low difference between the modeled structures containing the neutral and the cationic His385 residue, and reoptimized both structures. First, by comparison of the optimized structures of the native models 15 and 16, it could be observed that the protonation state of His385 has a negligible effect on the final position of the TI inside the native active site. Second, after comparison with the previous structures of the mutant models, it could be observed that there were only small displacements of the TI inside the active site in both models. This result, somewhat unexpected because of the aspartate longer and negatively charged side chain, indicates that Asp313 does not influence the orientation of the TI inside the active site. The distance between the closest carboxylate oxygen atom of Asp313 and the TI methyl carbon atom is relatively long, 3.74 Å in model 15 and 3.79 Å in model 16. As pointed out by Eschenburg et al., this distance is apparently too long for a direct attack of the carboxylate group on the TI methyl group, which suggests the intermediacy of another group, such as the hydroxyl group attached to C4 [9]. In fact, the carboxylate oxygen atom of Asp313 is accepting a hydrogen-bond from this hydroxyl group in the optimized models 15 and 16, with distances between the hydroxyl and the carboxylate oxygen atoms of 2.73 Å and 2.71 Å, respectively.

## 4. Conclusion

The presently modeled structures enabled the analysis of the TI interactions inside the EPSPS active site, including the positions of all hydrogen atoms, which could not be observed in the original D313A mutant enzyme structure. From the current modeling results, it can be concluded that after the TI formation in the enzyme active site, the His385 residue is most probably in neutral form and Lys22, Lys340, and Lys411 residues are in protonated form. By the study of acid-catalyzed EPSP hydrolysis, Clark and Berti have shown that EPSP was most reactive in its fully deprotonated form [32]. It is expected that EPSPS takes advantage from this fact by means of a strongly stabilizing environment for negative-charged species, which is in accordance with our modeling results indicating an active site containing three protonated lysine residues (besides three assumed protonated arginine residues).

The modeling of the native active site suggests that the protonation state of the His385 residue has only a minor effect on the TI position inside the active site. Asp313 is also unimportant for definition of the TI position inside the active site, which is probably determined by the strong interactions between the positive side chains of the lysine and arginine residues and the negative charged groups of the TI. Although there are alternative proposals in the literature [33], this residue was unequivocally showed by the results from Eschenburg et al. to be the base in the elimination step. Founded on a homology model of the native enzyme, Eschenburg et al. proposed that Asp313 should first abstract a proton from the 4-OH of S3P; then, the resulting oxyanion would abstract a proton from the C-3 of the PEP moiety [9]. The atomic distances observed in our models are in accordance with this proposal.

This result implicates an *anti* elimination process, because Asp313 is located on the opposite side of the leaving phosphate group. Biochemical analyses of the EPSPS reaction have provided strong evidence that addition and elimination proceed with opposite stereochemistry [34–36], so the addition of the S3P 5-OH group to C2 and of the proton to C3 of PEP should proceed in *syn* fashion. According to Eschenburg et al., the only acidic residue that is located on the same PEP face as the S3P 5-OH group is Lys22, in protonated form. Consequently, this residue should be *neutral* after the TI formation, which is in disagreement with our modeling results. More importantly, the Lys22 $N^{\zeta}$ atom is located near to the PEP C2 atom and not to C3 (see Fig. 3). Our results indicate that the Lys22 residue is in fact protonated, which is in accordance with the proposal that Lys22 could be a general acid catalyst for the TI breakdown [11,13]. In fact, besides participating in a hydrogen-bonding interaction with the carboxylate group of the TI PEP moiety (see Table 4), the Lys22 $N^{\zeta}$ atom also forms a strong hydrogen-bond with an oxygen atom of the leaving phosphate group ($N^{\zeta}$(Lys22)–O(phosphate) distance: 2.75 Å) in model 15. This hydrogen-bond could help the phosphate departure from the TI or the proton could be transferred to the leaving group, leading to a cationic intermediate (or cationic transition state).

Which residue could be the proton donor to PEP during an addition step in *syn* fashion? In our modeled structures, Lys340 is the nearest residue to the PEP methyl group that is on the same PEP face as the S3P 5-OH. A significant reduction in the EPSPS specific activity was observed as a consequence of the mutation of this residue to alanine [11]. However, there are two problems with this proposal: the distance between the Lys340 $N^{\zeta}$ atom and the methyl C atom is too long (4.34 Å in the native model 15), and, similar to Lys22, our results indicate that Lys340 is in protonated state after the TI formation. Nonetheless, differently from Lys22, the Lys340 $N^{\zeta}$ atom can become very close to the PEP C3 atom by simple rotations of the side chain C–C bonds. It is possible that after donating a proton to PEP, the Lys340 side chain has changed its conformation as a consequence of attractions by some of the nearest groups, such as the hydroxyl group connected to C4, the phosphate group attached to C3, a water molecule, and/or the carbonyl group of the Asn336 side chain. Is it also possible that some of these interactions resulted in a transfer of a proton to Lys340 after the TI formation, leading to the protonated state indicated by our modeling results?

In order to evaluate the participation of these residues in the reaction mechanism, a detailed and comparative study of the energetics of the catalyzed and uncatalyzed reactions is necessary. The results from this study will be presented

elsewhere. It must be remembered that our conclusions are based on experimental results that reflect a specific moment of the EPSP formation mechanism and that the protonation state could change when the enzyme is, for example, inhibited by glyphosate. Additional calculations will also be implemented for the study of the influence of the protonation state on the inhibition reaction.

## Acknowledgments

The Brazilian National Council of Research (CNPq) and the FAPERJ Foundation are acknowledged for financial support and fellowship (to CMRS).

LASSBio/UFRJ is acknowledged for the use of Spartan'02 for Linux program.

## References

[1] F. Roberts, C.W. Roberts, J.J. Johnson, D.E. Kyle, T. Krell, J.R. Coggins, G.H. Coombs, W.K. Milhous, S. Tzipori, D.J. Ferguson, D. Chakrabarti, R. Mcleod, Nature 393 (1998) 801–805.
[2] H.C. Steinrücken, N. Amrhein, Biochem. Biophys. Res. Commun. 94 (1980) 1207–1212.
[3] E. Schönbrunn, S. Eschenburg, W.A. Shuttleworth, J.V. Schloss, N. Amrhein, J.N.S. Evans, W. Kabsch, Proc. Natl. Acad. Sci. USA 98 (2001) 1376–1380.
[4] D.L. Anton, L. Hedstrom, S.M. Fish, R.H. Abeles, Biochemistry 22 (1983) 5903–5908.
[5] D.R. Studelska, L.M. McDowell, M.P. Espe, C.A. Klug, J. Schaefer, Biochemistry 36 (1997) 15555–15560.
[6] K.S. Anderson, J.A. Sikorski, A.J. Benesi, K.A. Johnson, J. Am. Chem. Soc. 110 (1988) 6577–6579.
[7] D.L. Jakeman, D.J. Mitchell, W.A. Shuttleworth, J.N.S. Evans, Biochemistry 37 (1998) 12012–12019.
[8] J. Lewis, K.A. Johnson, K.S. Anderson, Biochemistry 38 (1999) 7372–7379.
[9] S. Eschenburg, W. Kabsch, M.L. Healy, E. Schönbrunn, J. Biol. Chem. 278 (2003) 49215–49222.
[10] W.A. Shuttleworth, M.E. Pohl, G.L. Helms, D.L. Jakeman, J.N.S. Evans, Biochemistry 38 (1999) 296–302.
[11] S. Mizyed, J.E.I. Wright, B. Byczynski, P.J. Berti, Biochemistry 42 (2003) 6986–6995.
[12] L.M. McDowell, D.R. Studelska, B. Poliks, R.D. O'Connor, J. Schaefer, Biochemistry 43 (2004) 6606–6611.
[13] B. Byczynski, S. Mizyed, P.J. Berti, J. Am. Chem. Soc. 125 (2003) 12759–12767.
[14] G.F. Signorini, R. Chelli, P. Procacci, V. Schettino, J. Phys. Chem. B 108 (2004) 12252–12257.
[15] F.D. González-Nilo, H. Krautwurst, A. Yévenes, E. Cardemil, R. Cachau, Biochim. Biophys. Acta 1599 (2002) 65–71.
[16] M.J.S. Dewar, E.G. Zoebish, E.F. Healy, J.J.P. Stewart, J. Am. Chem. Soc. 107 (1985) 3902.
[17] J.J.P. Stewart, J. Comp. Chem. 10 (1989) 209–220.
[18] J.J.P. Stewart, J. Comp. Chem. 10 (1989) 221–264.
[19] S. Schröder, V. Daggett, P. Kollman, J. Am. Chem. Soc. 113 (1991) 8922–8925.
[20] Y.-J. Zheng, K.M. Merz Jr., J. Comp. Chem. 13 (1992) 1151–1169.
[21] M.W. Jurema, G.C. Shields, J. Comp. Chem. 14 (1993) 89–104.
[22] T.N. Lively, M.W. Jurema, G.C. Shields, Int. J. Quant. Chem., Quant. Biol. Symp. 21 (1994) 95–107.
[23] A.K. Katz, X. Li, H.L. Carrell, B.L. Hanson, P. Langan, L. Coates, B.P. Schoenborn, J.P. Glusker, G.J. Bunick, Proc. Natl. Acad. Sci. USA 103 (2006) 8342.
[24] A.A. Kossiakoff, Basic Life Sci. 27 (1984) 281–304.
[25] R. Sayle, Glaxo Wellcome Research and Development, Stevenage, Hertfordshire, UK, 1993.
[26] P. Walters, M. Stahl, University of Arizona, USA, 1992.
[27] J.J.P. Stewart, QCPE 455, Available from Indiana University, Bloomington, USA, 1992.
[28] J.J.P. Stewart, Int. J. Quant. Chem. 58 (1996) 133–146.
[29] C.M.R. Sant'Anna, A.S. Viana, N.M. Nascimento Junior, Bioorg. Chem. 34 (2006) 77–89.
[30] V.M.R. Santos, C.M.R. Sant'Anna, G.E. Moya Borja, A. Chaaban, W.S. Côrtes, J.B.N. DaCosta, Bioorg. Chem. 35 (2007) 68–81.
[31] A. Klamt, G. Schüürmann, J. Chem. Soc. Perkin Trans. 2 (1993) 799–805.
[32] M.E. Clark, P.J. Berti, Biochemistry 46 (2007) 1933–1940.
[33] M. An, U. Maitra, U. Neidlein, P.A. Bartlett, J. Am. Chem. Soc. 125 (2003) 12759–12767.
[34] C.E. Grimshaw, S.G. Sogo, J.R. Copley, S.D. Knowles, J. Am. Chem. Soc. 106 (1984) 2699–2700.
[35] J.J. Lee, Y. Asano, T.-L. Shieh, F. Spreafico, K. Lee, H.G. Floss, J. Am. Chem. Soc. 106 (1984) 3367–3368.
[36] W.J. Lees, C.T. Walsh, J. Am. Chem. Soc. 117 (1995) 7329–7337.